RSC Advances

PAPER

View Article Online
View Journal | View Issue

Cite this: *RSC Adv.*, 2022, **12**, 5483

Non-metal-mediated *N*-oxyl radical (TEMPO)-induced acceptorless dehydrogenation of N-heterocycles *via* electrocatalysis†

Huiqing Hou,‡[a] Xinhua Ma,‡[a] Yaling Ye,[a] Mei Wu,[a] Sunjie Shi,[a] Wenhe Zheng,[b] Mei Lin,[a] Weiming Sun *[a] and Fang Ke *[a]

Received 8th December 2021
Accepted 1st February 2022

DOI: 10.1039/d1ra08919f

rsc.li/rsc-advances

The development of protocols for direct catalytic acceptorless dehydrogenation of N-heterocycles with metal-free catalysts holds the key to difficulties in green and sustainable chemistry. Herein, an *N*-oxyl radical (TEMPO) acting as an oxidant in combination with electrochemistry is used as a synthesis system under neutral conditions to produce N-heterocycles such as benzimidazole and quinazolinone. The key feature of this protocol is the utilization of the TEMPO system as an inexpensive and easy to handle radical surrogate that can effectively promote the dehydrogenation reaction. Mechanistic studies also suggest that oxidative TEMPOs redox catalytic cycle participates in the dehydrogenation of 2,3-dihydro heteroarenes.

Catalytic acceptorless dehydrogenation (CAD) is an important reaction in which hydrogen is liberated to change the substrate.[1] In terms of atom-economy and waste generation, this approach has obvious advantages compared with traditional methods using stoichiometric amounts of oxidant or sacrificial hydrogen acceptors. In addition, acceptorless dehydrogenative coupling condensation of substituted alcohols with *o*-substituted anilines is an atom-economical and environmentally friendly method for the construction of new C–N bonds,[2] which has recently emerged as an important process to afford many useful organic compounds such as imines, amides, amines, or nitrogen-containing heterocyclic compounds.[3]

Toward this direction, acceptorless dehydrogenation is mainly catalysed by transition metal catalysts by the liberation of hydrogen gas without the use of stoichiometric oxidants in the process.[4] In 1981, an initial example of *N*-alkylation of alcohols by using a variety of amines *via* dehydrogenative coupling was showcased by Watanabe which required a noble metal catalyst ruthenium as $RuCl_2(PPh_3)_3$ at a very high temperature of >200 °C.[5] More recently, Fujita and coworkers reported the first catalytic system for the reversible dehydrogenation/hydrogenation of quinoline derivatives using an iridium-based complex in 2009.[6] What is more, several of metal-free catalyst representatives for this important transformation of diamines and alcohols have been reported.[7] In 2019, Malakar and co-workers demonstrated the metal-free 3-nitropyridine-catalyzed facile synthesis of 2-functionalized benzoxazoles, naphthoxazoles, benzothiazoles and benzimidazoles at 110 °C.[7a] In contrast, although significant advances have been made in metal- or metal-free-catalyzed acceptorless dehydrogenation, the use of metal complexes with multistep synthesized ligands or harsh catalytic conditions has restricted its applicability on large scales. From the standpoint of sustainable chemistry, the development of a new mild strategy *via* CAD from easily available starting materials is highly desirable.

Nitroxyl radicals are *N*,*N*-disubstituted NO radicals with an unpaired delocalized electron.[8] These open-shell species have diverse reactivity and can undergo reactions such as a single-electron transfer (SET) to access three discrete oxidation states (*i.e.*, $TEMPO^-$/TEMPO/$TEMPO^+$) or abstract hydrogen atoms from C–H/X–H bonds.[9] Transition metals such as ruthenium, rhodium, palladium or copper with the assistance of co-catalyst TEMPO have been proved efficient co-catalysts, and have been utilized to CAD.[10] More recently, TEMPO has been extensively used as a catalyst cooperating with electrocatalysis in CAD which is a green and atom-economical alternative.[11] In general, the electrochemical reaction with electrons as the oxidizing/reducing agent can be performed at room temperature without the use of chemical oxidants, which makes it safe and low cost.[12] Recently, Gong's group has developed an electrochemical dehydrogenation method for synthesis of quinazolin-4(3*H*)-ones under metal-free and oxidant-free conditions by combining acid-catalyzed annulation and TEMPO as the catalyst.[11b] Inspired by the Gong work, we envisaged electrocatalysis

[a]*School of Pharmacy, Fujian Provincial Key Laboratory of Natural Medicine Pharmacology, Fujian Medical University, Fuzhou 350004, China. E-mail: kefang@mail.fjmu.edu.cn; Fax: +86-591-22862016; Tel: +86-591-22862016*

[b]*The First Affiliated Hospital of Fujian Medical University, Fuzhou 350004, China*

† Electronic supplementary information (ESI) available. See DOI: 10.1039/d1ra08919f

‡ These authors contributed equally to this work.

combined with nitroxyl radicals as a new strategy to direct catalytic acceptorless dehydrogenation of N-heterocycles under neutral conditions (Scheme 1).

Furthermore, our previous reports on electrochemical synthesis show high reactivity for acceptorless dehydrogenation of primary alcohols to aldehydes.[13] Therefore, simultaneous electron transfer and TEMPO-induced chemical reaction is a powerful tool to realize highly selective and relatively environmentally friendly CAD. Herein, we report such a reaction catalyzed by TEMPO to selectively generate nitrogen heterocycles under neutral conditions, with the evolution of H_2 as the only byproduct.

In the preliminary studies, benzyl alcohol and *o*-phenylenediamine were selected as the substrates in MeCN/H_2O solvent in the presence of the catalyst TEMPO (0.2 equiv.) and electrolyte tetrabutylammonium hexafluorophosphate ($TBAPF_6$, 0.15 M) to produce a 93% yield of **3aa** at constant current (80 mA) at room temperature. As illustrated in Table 1, entries 1–5 show that related nitroxyl derivatives were important catalysts for electrochemical CAD of the catalysts examined, but TEMPO exhibited the highest performance. This may be due to the introduction of an electron-donating group reducing the electron acquisition capacity of the TEMPO cation, leading to difficulty in dehydrogenation of 2,3-dihydro heteroarenes. A change of the electrolyte from $TBAPF_6$ to tetrabutylammonium bromide (TBAB) or tetrabutylammonium iodide (TBAI) led to a decrease of the product yield (Table 1, entries 6 and 7). These results showed that the role of the halogen salts was not only as the electrolyte, but also as a redox mediator which competes to inhibit TEMPO oxidation. Further investigative experiments indicated that the product yield decreased when single or mixed solvents DMSO, DMF, THF, 1.4-dioxane and/or H_2O were used instead of MeCN, indicating that MeCN/H_2O was superior to the other solvents (Table 1, entries 8–12). The solvent effect may be

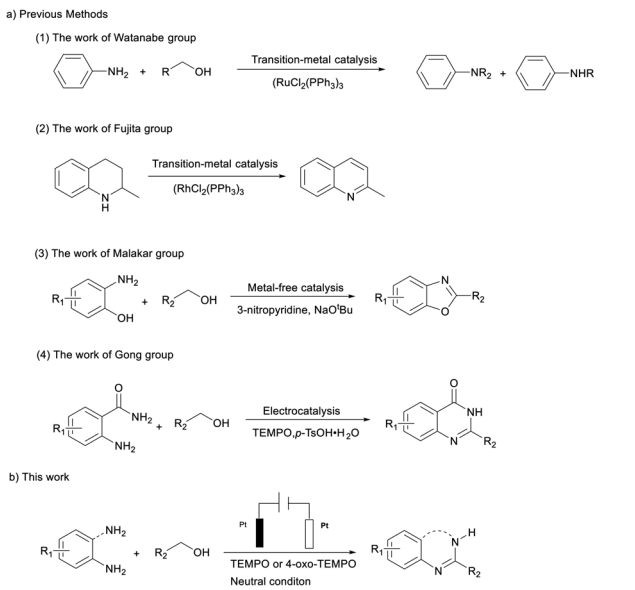

Scheme 1 Methods for acceptorless dehydrogenative reactions.

Table 1 Optimization of the reaction conditions of benzimidazole[a]

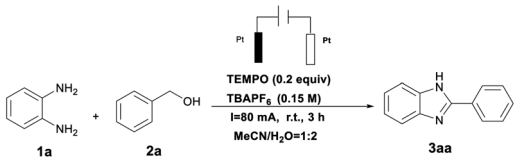

Entry	Variations from the standard conditions	Yield[b] (%)
1	**None**	**93**
2	4-Amino-TEMPO instead of TEMPO	57
3	4-Hydroxy-TEMPO instead of TEMPO	64
4	4-Oxo-TEMPO instead of TEMPO	58
5	No TEMPO	Trace
6	TBAB instead of $TBAPF_6$	36
7	TBAI instead of $TBAPF_6$	23
8	DMSO/H_2O (v/v = 1 : 2) as solvent	76
9	DMF/H_2O (v/v = 1 : 2) as solvent	33
10	THF/H_2O (v/v = 1 : 2) as solvent	46
11	1,4-Dioxane/H_2O (v/v = 1 : 2) as solvent	Trace
12	H_2O as solvent	73
13	No current	Trace
14	40 mA	49
15	60 mA	64
16	C (+)/Pt (−)	31
17	5 h	92

[a] Standard conditions: undivided cell, Pt anode (1.0 cm × 1.0 cm), Pt cathode (1.0 cm × 1.0 cm), **1a** (0.5 mmol), **2a** (0.8 mmol), TEMPO (0.1 mmol), $TBAPF_6$ (0.15 M), CH_3CN/H_2O (v/v = 1 : 2, 3 mL), I = 80 mA at room temperature for 3 h. [b] Isolated yield.

related to the conductivity of the system. A decrease in electrical conductivity results in a decrease in yield. 1.4-Dioxane diminished the conductivity of the system drastically and hence did not yield **3aa**. Moreover, organic compounds had poor solubility in H_2O, leading to conductivity issues, and thus produced inferior yields of **3aa**. We next turned our attention to investigating the effect of current on the yield. Decreased or trace desired produced was formed if the reaction was conducted at reduced or in the absence of current (Table 1, entries 13–15). When the reaction was conducted at lower constant current (40 and 60 mA), there was an obvious decrease in the yields (Table 1, entries 14 and 15). A decrease in current leads to a decrease in current density, which results in differing concentrations of electron oxidation products, inhibiting further oxidation of **2a**. It was also noteworthy that when the Pt electrodes were replaced by graphite rods, the product yield was 31% (Table 1, entry 16). In addition, the discrepancy in reactivity between graphite electrode and Pt electrode may cause a difference in current density at the anode surface, which results in decreasing the rate of electron transfer as well. It was noted that increasing the time for reaction had little effect on the yield (Table 1, entry 17).

With the optimal reaction conditions established, we next explored the generality of this protocol for the synthesis of N-heterocyclic compounds. As illustrated in Table 2, a variety of benzyl alcohols with electron-withdrawing or electron-donating groups were well tolerated and gave the corresponding products

Table 2 Substrate scope for electrochemical synthesis of benzimidazole derivatives[a,b]

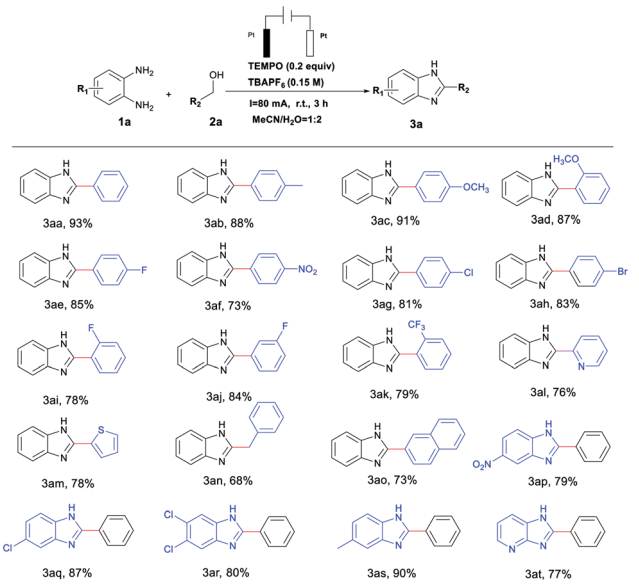

[a] Reaction conditions: undivided cell, Pt anode (1.0 cm × 1.0 cm), Pt cathode (1.0 cm × 1.0 cm), **1a** (0.5 mmol), **2a** (0.8 mmol), TEMPO (0.1 mmol), $TBAPF_6$ (0.15 M), CH_3CN/H_2O (v/v = 1 : 2, 3 mL), constant current 80 mA, under air at room temperature for 3 h. [b] Isolated yield.

Table 3 Substrate scope for electrochemical synthesis of quinazolinone derivatives[a,b]

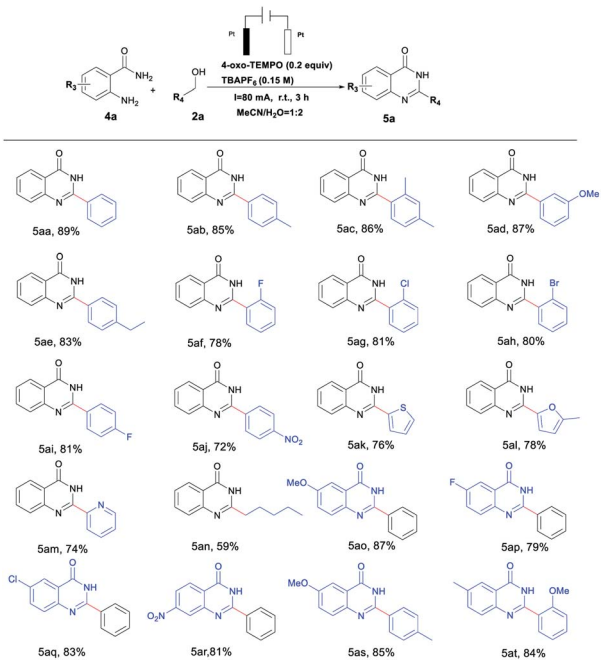

[a] Reaction conditions: undivided cell, Pt anode (1.0 cm × 1.0 cm), Pt cathode (1.0 cm × 1.0 cm), **1a** (0.5 mmol), **2a** (0.8 mmol), 4-oxo-TEMPO (0.1 mmol), $TBAPF_6$ (0.15 M), CH_3CN/H_2O (v/v = 1 : 2, 3 mL), constant current 80 mA, under air at room temperature for 3 h. [b] Isolated yield.

in good to excellent yields (**3aa–3ak**). Compared with electron-donating groups, electron-withdrawing groups (–NO_2, –F, –Cl, –Br, –CF_3) resulted in a relatively medium yield of 73–85% (Table 2, **3af–3ak**). Heterocyclic alcohols (pyridinyl and thienyl) also proved to be good substrates for this process, giving good yields of benzazoles under similar conditions (**3al** and **3am**). Notably, we were pleased to find an aliphatic alcohol (phenylethanol) could deliver the desired benzimidazole derivatives in a good yield of 68% (**3an**). An alcohol bearing a naphthyl group also participated in this reaction with high reactivity to afford the desired product in 73% yield (**3ao**). On the other hand, various substituted *o*-phenylenediamines were employed and the reaction proceeded successfully with a yield range of 79–90% (Table 2, **3ap–3at**). Similar to the observations in for substituted alcohol compounds, *o*-phenylenediamine with electron-donating groups (–Me) gave relatively higher reactivity than those with electron-withdrawing (–Cl, and –NO_2) ones (**3ap–3as**). Moreover, challenging substrates like pyridine-2,3-diamine also furnished the desired pteridin-4(3*H*)-one in 77% yield (Table 2, **3at**).

Interestingly, quinazolinone derivatives could also be reached in excellent yields by tuning reaction conditions to investigate use of 4-oxo-TEMPO as the catalyst, which are summarized in Table 3. It was observed that *o*-aminobenzamides or benzyl alcohols bearing various functional groups could be smoothly converted to the desired products in yields of 59–89%; not coincidentally, aminobenzamides or benzyl alcohols with electron-donating groups (–Me, –OMe or ethyl) gave relatively higher reactivity than those with electron-withdrawing (–F, –Cl or –Br) ones (Table 3, **5ab–5aj**, **5ao–5at**). In addition, heterocyclic alcohols and amides, and long-chain aliphatic alcohols were also well-tolerated in this catalytic system (Table 3, **5ak–5an**).

In order to understand the reaction mechanism, several control experiments were carried out, as shown in Scheme 2. When **2a** was subjected to the standard conditions, 75% and 72% yields of **6a** were detected (Scheme 2(a)), while the yield of **6a** was decreased to 22% or trace in the absence of catalyst or current (Scheme 2(b)). Comparing Scheme 2(c) and (d), we found that when **6a** was added to the reaction system in the absence of catalyst, a decreased amount of **3aa** was separated from the reaction mixture. This pretty obviously indicated that TEMPO still plays an important role after **1a** and **6a** are conjured to form intermediates. Furthermore, a similar scenario appears in the synthesis of quinazolinone compounds (Scheme 2(e) and (f)).

When the radical inhibitor 2,6-di-*tert*-butyl-4-methylphenol (BHT) was added under standard conditions this transformation process was inhibited to a large degree (Scheme 3), which implies that the reaction goes through a radical process.

To gain an understanding of the reaction mechanism, cyclic voltammetry (CV) was then conducted (Fig. 1). By comparing CV curves a, and b (Fig. 1A), we observed that the TEMPO showed an oxidation peak at E_p = +1.50 V *vs.* SCE and a reduction peak at E_p = +0.34 V *vs.* SCE, while the peak changed slightly after the

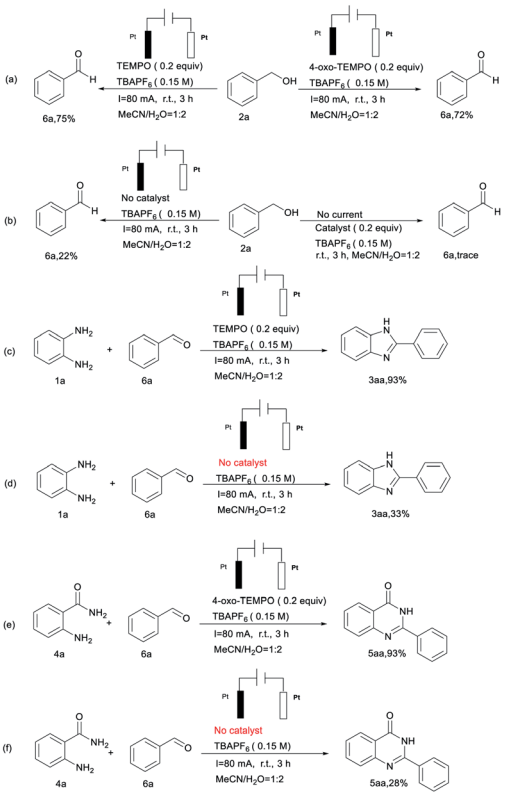

Scheme 2 Control experiments.

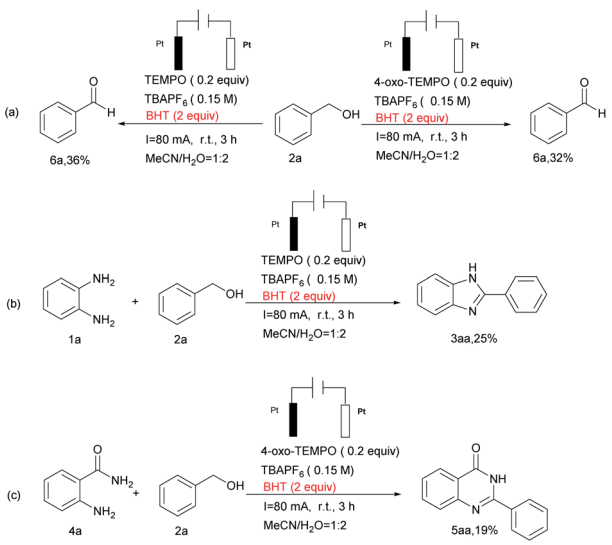

Scheme 3 Radical trapping experiments.

addition of **2a**. These results indicate that both TEMPO and current together are required, to participate in the redox process of **2a**. Furthermore, the mixture of **1a** and **2a** resulted in the appearance of a small curvilinear trend in comparison with that of curve d (Fig. 1B, curves c and d), which indicates that current and TEMPO act in coordination to promote further reactions of **1a** and **2a**. Furthermore, a similar curvilinear trend appears in the cyclic voltammetry of quinazolinones (ESI Fig. 1C and D†).

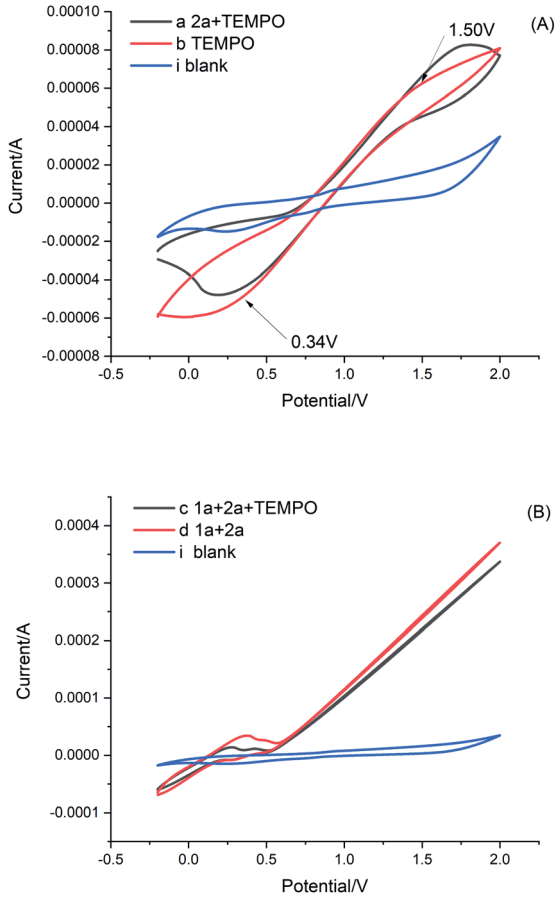

Fig. 1 Cyclic voltammograms of reactants and their mixtures in 0.15 M $TBAPF_6/CH_3CN$: H_2O (1 : 2) on a Pt disk working electrode (diameter: 3 mm) with a Pt wire and calomel electrode as the counter and reference electrode, respectively, at a scan rate of 0.1 V s^{-1}.

On the basis of the above results and the previous reports, a possible mechanism is provided in Scheme 4.[14–17] We envisioned that the reaction proceeds initially through an oxidative redox cycle between TEMPO/4-oxo-TEMPO to $TEMPO^+$/4-oxo-$TEMPO^+$, which promotes the conversion of **2a** to **A**.[14] The consequent deprotonation of the radical cation **A** results in the formation of benzylic radical **B**. The following fast single-electron oxidation to **C** and its subsequent deprotonation produce the desired benzaldehyde (**6a**). In the meantime, water undergoes cathodic reduction to generate hydroxide accompanied by releasing hydrogen.[15] Afterwards, as shown in pathway 1, **6a** can readily react with **1a** to obtain the imine **D1**, then imine **D1** is converted to **E1** which is oxidized (dehydrogenated) to afford the desired product **3aa** *via* a radical-cation intermediate **F1**.[16] Similarly, hexagonal nitrogen-containing heterocyclic ring **6a** also works well in the same way as shown in pathway 2.[17]

To gain a better understanding of the details of the reaction mechanism, density functional theory (DFT) calculations were performed, and the obtained energy profiles are plotted in Fig. 2. DFT results suggested the formation of the phenylmethanol radical **B** ($^{\bullet}C_6H_5CH_2OH$) and $TEMPO^+$ *via* electron transfer from **2a** to $TEMPO^+$ with an activation energy barrier of +34.83 kcal mol^{-1}.

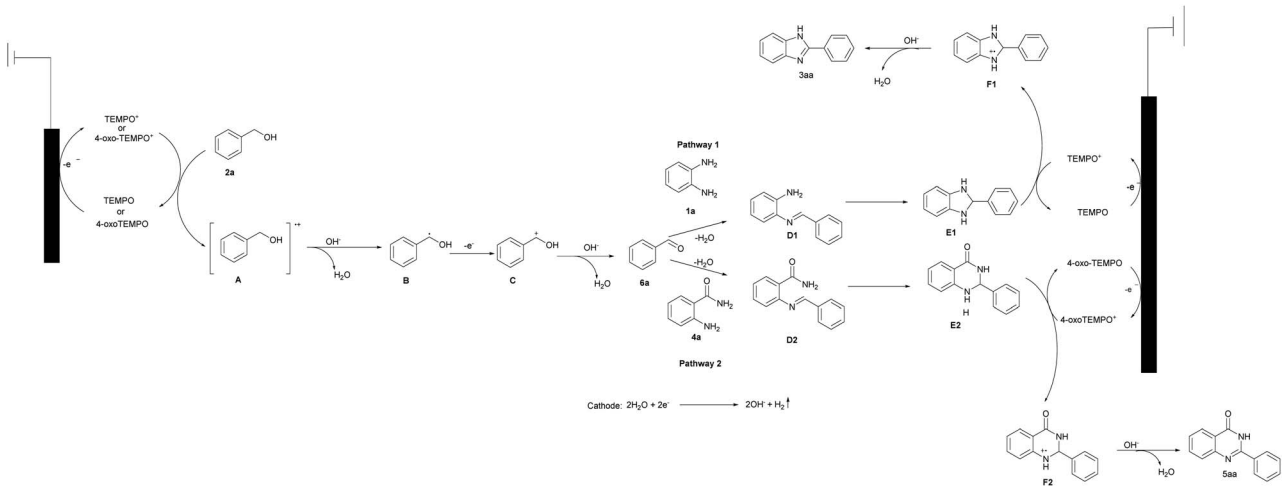

Scheme 4 Proposed mechanism for this transformation.

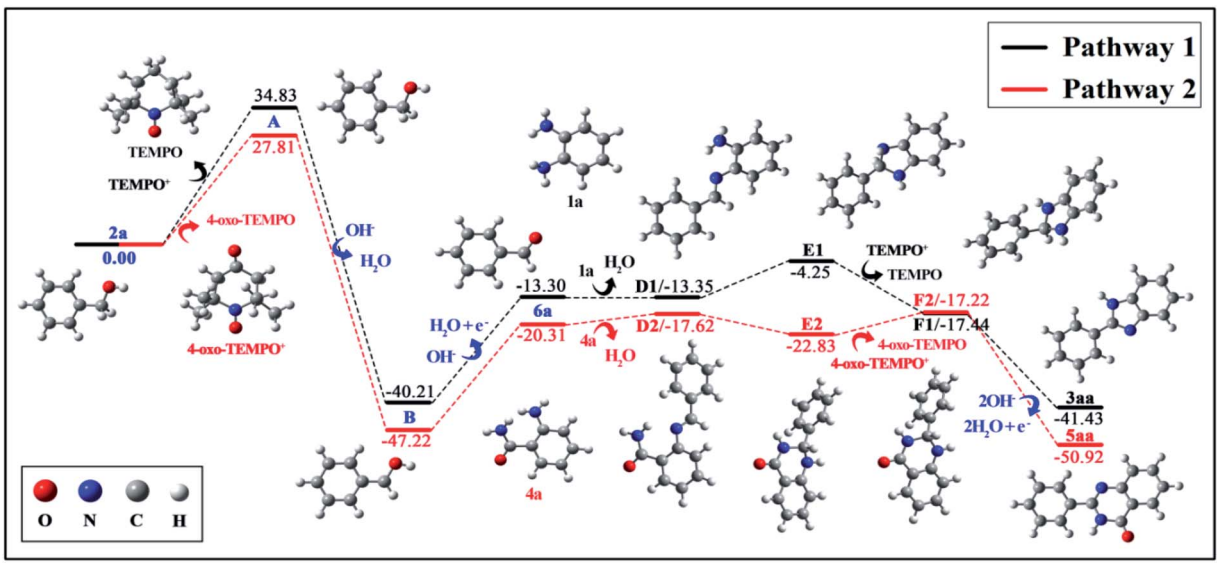

Fig. 2 Computed energy profiles for the oxidative cyclization of nitrogen-containing heterocycles.

Similarly, 4-oxo-TEMPO can also promote the change from **2a** to **B** with an energy barrier of +27.81 kcal mol^{-1}. Afterwards, the resulting radical **B** will form **6a** *via* single-electron oxidation by absorbing energy of +26.91 kcal mol^{-1} both in pathway 1 and in pathway 2, indicating that both 4-oxo-TEMPO^{+} and TEMPO^{+} can catalyze the transition from **2a** to **6a**. Subsequently, **6a** can easily react with **1a** and **4a** to generate **D1** and **D2**. And then, imine **D** is converted to radical-cation **F** *via* a loop-locked intermediate **E** under the catalysis of TEMPOs. Obviously, this step only has a very low energy barrier of 9.10 kcal mol^{-1} to overcome for **D1**, and no energy barrier for **D2**. Finally, the deprotonation of **F1** and **F2** yields the desired products **3aa** and **5aa**, along with releasing energy of −23.99 kcal mol^{-1} and −33.70 kcal mol^{-1}, respectively. In total, this TEMPO catalysis system is suitable for the oxidative cyclization of nitrogen-containing heterocycles from the viewpoint of thermodynamics and chemical kinetics.

Conclusions

In summary, an efficient electrocatalytic reaction *via* catalytic acceptorless dehydrogenation of a range of activated N-heterocycles has been developed using commercially available TEMPOs acting as oxidants under neutral conditions. Importantly, the present method employs a low-cost, environmentally friendly electrocatalyst and avoids using a metal catalyst. This catalysis system is of great value for oxidative cyclization of nitrogen-containing heterocycles from the viewpoint of green chemistry and organic synthesis. Moreover, DFT calculations were also performed to verify the mechanism that we proposed and to prove this system is suitable for the formation of *N*-heterocycles. Further synthetic application of this reaction for the efficient synthesis of various heterocyclic compounds is currently under investigation.

Conflicts of interest

There are no conflicts to declare.

Acknowledgements

This work was supported by Fujian Provincial Foundation (Nos. 2020R1012-1, FJNMP-201902, FJNMP-2020004, 2019R11020034-1, 2020J01622, 2020J01627, and 2018QH2021).

Notes and references

1 (*a*) M. Zheng, J. Shi and T. Yuan, *Angew Chem., Int. Ed.*, 2018, **57**, 5487–5491; (*b*) P. Ryabchuk, A. Agapova, C. Kreyenschulte, H. Lund, H. Junge, K. Junge and M. Beller, *Chem. Commun.*, 2019, **55**, 4969–4972; (*c*) T. liu, K. Wu, L. Wang and Z. Yu, *Adv. Synth. Catal.*, 2019, **361**, 3958–3964; (*d*) G. A. Filonenko, R. van Putten, E. J. M. Hensen and E. A. Pidko, *Chem. Soc. Rev.*, 2018, **47**, 1459–1483; (*e*) P. Preuster, C. Papp and P. Wasserscheid, *Acc. Chem. Res.*, 2017, **50**, 74–85; (*f*) R. H. Crabtree, *ACS Sustainable Chem. Eng.*, 2017, **5**, 4491–4498.

2 (*a*) H. Song, B. Kang and S. H. Hong, *ACS Catal.*, 2014, **4**, 2889–2895; (*b*) K.-N. T. Tseng, A. M. Rizzi and N. K. Szymcza, *J. Am. Chem. Soc.*, 2013, **135**, 16352–16355; (*c*) S. Xu, L. M. Alhthlol, K. Paudel, E. Reinheimer, D. L. Tyer, D. K. Taylor, A. M. Smith, J. Holzmann, E. Lozano and K. Ding, *Inorg. Chem.*, 2018, **57**, 2394–2397.

3 (*a*) W. Zhao, P. Liu and F. Li, *ChemCatChem*, 2016, **8**, 1523–1530; (*b*) B. Saha, S. M. W. Rahaman, P. Daw, G. Sengupta and J. K. Bera, *Chem.–Eur. J.*, 2014, **20**, 6542–6551; (*c*) S. K. Patra and J. K. Bera, *Organometallics*, 2007, **26**, 2598–2603.

4 (*a*) E. Clot, O. Eisenstein and R. H. Crabtree, *Chem. Commun.*, 2007, 2231–2233; (*b*) X. Cui, Y. Li, S. Bachmann, M. Scalone, A.-E. Surkus, K. Junge, C. Topf and M. Beller, *J. Am. Chem. Soc.*, 2015, **137**, 10652–10658; (*c*) K. He, F. Tan, C. Zhou, G. Zhou, X. Yang and Y. Li, *Angew. Chem., Int. Ed.*, 2017, **56**, 3080–3084; (*d*) S. P. Midya, V. G. Landge, M. K. Sahoo, J. Rana and E. Balaraman, *Chem. Commun.*, 2018, **54**, 90–93; (*e*) M. Mastalir, G. Tomsu, E. Pittenauer, G. Allmaier and K. Kirchner, *Org. Lett.*, 2016, **18**, 3462–3465; (*f*) G. Zhang, J. Wu, H. Zeng, S. Zhang, Z. Yin and S. Zheng, *Org. Lett.*, 2017, **19**, 1080–1083.

5 Y. Watanabe, Y. Tsuji and Y. Ohsugi, *Tetrahedron Lett.*, 1981, **22**, 2667–2670.

6 R. Yamaguchi, C. Ikeda, Y. Takahashi and K. Fujita, *J. Am. Chem. Soc.*, 2009, **131**, 8410–8412.

7 (*a*) D. Kaldhi, N. Vodnala, R. Gujjarappa, S. Nayak, V. Ravichandiran, S. Gupta, G. K. Hazraa and C. C. Malakar, *Tetrahedron Lett.*, 2019, **60**, 223–229; (*b*) G. M. Raghavendra, A. B. Ramesha, C. N. Revanna, K. N. Nandeesh, K. Mantelingu and K. S. Rangappa, *Tetrahedron Lett.*, 2011, **52**, 5571–5574.

8 (*a*) T. Vogler and A. Studer, *Synthesis*, 2008, **13**, 1979–1993; (*b*) H. Lv, R. D. Laishram, Y. Yang, J. Li, D. Xu, Y. Zhan, Y. Luo, Z. Su, S. More and B. Fan, *Org. Biomol. Chem.*, 2020, **18**, 3471–3474; (*c*) N. O. Balayeva, N. Zheng, R. Dillert and D. W. Bahnemann, *ACS Catal.*, 2019, **9**, 10694–10704; (*d*) D. Griller and K. U. Ingold, *Acc. Chem. Res.*, 1976, **9**, 13–19; (*e*) L. Tebben and A. Studer, *Angew. Chem., Int. Ed.*, 2011, **50**, 5034–5068.

9 (*a*) J.-L. Zhan, M.-W. Wu, D. Wei, B.-Y. Wei, Y. Jiang, W. Yu and B. Han, *ACS Catal.*, 2019, **9**, 4179–4188; (*b*) J. C. Siu, G. S. Sauer, A. Saha, R. L. Macey, N. Fu, T. Chauvire, K. M. Lancaster and S. Lin, *J. Am. Chem. Soc.*, 2018, **140**, 12511–12520.

10 (*a*) J. Yu, J. Xu and M. Lu, *Appl. Organomet. Chem.*, 2013, **27**, 606–610; (*b*) Z.-G. Wang, X.-H. Cao, Y. Yang and M. Lu, *Synth. Commun.*, 2015, **45**, 1476–1483.

11 (*a*) Y. Wu, H. Yi and A. Lei, *ACS Catal.*, 2018, **8**, 1192–1196; (*b*) L. Cao, H. Huo, H. Zeng, Y. Yu, D. Lu and Y. Gong, *Adv. Synth. Catal.*, 2018, **360**, 4764–4773; (*c*) Y.-L. Lai, J.-S. Ye and J.-M. Huang, *Chem.–Eur. J.*, 2016, **22**, 5425–5429; (*d*) N. Sbei, A. V. Listratova, A. A. Titov and L. G. Voskressensky, *Synthesis*, 2019, **51**, 2455–2473.

12 (*a*) P.-F. Zhang, H.-M. Lin, L.-W. Wang, Z.-Y. Mo, X.-J. Meng, H.-T. Tang and Y.-M. Pan, *Green Chem.*, 2020, **22**, 6334–6339; (*b*) P.-S. Gao, X.-J. Weng, Z.-H. Wang, C. Zheng, B. Sun, Z.-H. Chen, S.-L. You and T.-S. Mei, *Angew. Chem., Int. Ed.*, 2020, **59**, 15254–15259; (*c*) J.-Y. Chen, H.-Y. Wu, Q.-W. Gui, S.-S. Yan, J. Deng, Y.-W. Lin, Z. Cao and W.-M. He, *Chin. J. Catal.*, 2021, **42**, 1445–1450; (*d*) J. P. Barham and B. Konig, *Angew. Chem., Int. Ed.*, 2020, **59**, 11732–11747; (*e*) H. Ding, K. Xu and C.-C. Zeng, *J. Catal.*, 2020, **381**, 38–43; (*f*) H.-T. Tang, J.-S. Jia and Y.-M. Pan, *Org. Biomol. Chem.*, 2020, **18**, 5315–5333; (*g*) Y. Wu, J.-Y. Chen, J. Ning, X. Jiang, J. Deng, Y. Deng, R. Xu and W.-M. He, *Green Chem.*, 2021, **23**, 3950–3954.

13 (*a*) H. Hou, X. Ma, Y. Lin, J. Lin, W. Sun, L. Wang, X. Xu and F. Ke, *RSC Adv.*, 2021, **11**, 17721–17726; (*b*) Y. Hu, H. Hou, L. Yu, S. Zhou, X. Wu, W. Sun and F. Ke, *RSC Adv.*, 2021, **11**, 31650–31655; (*c*) L. Yang, H. Hou, L. Li, J. Wang, S. Zhou, M. Wu and F. Ke, *Org. Biomol. Chem.*, 2021, **19**, 998–1003.

14 J. E. Nutting, M. Rafiee and S. S. Stahl, *Chem. Rev.*, 2018, **118**, 4834–4885.

15 (*a*) D. Wang, P. Wang, S. Wang, Y.-H. Chen, H. Zhang and A. Lei, *Nat. Commun.*, 2019, **10**, 2796–2804; (*b*) R. Rajeev, B. Sharma, A. T. Mathew, L. Groege, Y. N. Sudhakar and A. Varghese, *J. Electrochem. Soc.*, 2020, **167**, 136508–136526.

16 (*a*) K. Tateyama, K. Wada, H. Miura, S. Hosokawa, R. Abe and M. Inoue, *Catal. Sci. Technol.*, 2016, **6**, 1677–1684; (*b*) A. Ziarati, A. Baadiei, G. M. Ziarani and H. Eskandarloo, *Catal. Commun.*, 2017, **95**, 77–82; (*c*) Q. An, C. He, X. Fan, C. Hou, J. Zhao, Y. Liu, H. Liu, J. Ma, Z. Sun and W. Chu, *ChemElectroChem*, 2020, **7**, 3969–3974.

17 (*a*) Y. Hu, S. Li, H. Li, Y. Li, J. Lin, C. Duanmu and B. Li, *Org. Chem. Front.*, 2019, **6**, 2744–2748; (*b*) M. Kumar, Richa, S. Sharma, V. Bhatt and N. Kumar, *Adv. Synth. Catal.*, 2015, **357**, 2862–2868; (*c*) Q. Wang, M. Lv, J. Liu, Y. Lo, H. Cao, X. Zhang and Q. Xu, *ChemSusChem*, 2019, **12**, 3043–3048.